Journal of the Serbian Chemical Society
JSCS-info@shd.org.rs • www.shd.org.rs/JSCS
J. Serb. Chem. Soc. 78 (10) 1609–1616 (2013)
JSCS–4522
UDC *Doxorubicin+547.391.1+546.723'722:615.277
Original scientific paper

Preparation and *in vitro* drug delivery response of doxorubicin-loaded poly(acrylic acid)-coated magnetite nanoparticles

REYHAN OMIDIRAD*, FARZANEH HOSSEINPOUR RAJABI and BAHMAN VASHEGHANI FARAHANI

Department of Chemistry, Faculty of Science, Imam Khomeini International University, Qazvin, Iran

(Received 25 December 2012, revised 12 March 2013)

Abstract: In this study, spherical superparamagnetic iron oxide nanoparticles (SPION) with mean diameter of 6 nm were prepared by a reduction–precipitation method. The surface of SPION were coated with poly(acrylic acid) 5000 (PAA-5000) and followed by loading with the anticancer drug doxorubicin (DOX). The drug loading efficiency was (14.64±0.29). *In vitro* drug release studies were realized for 8 h at two different pH values 4.2 and 7.4. The drug release rate at pH 4.2 (100 % DOX released in 2 h) was much faster than that at pH 7.4 (≈78 % DOX released in 8 h). These results indicate that these DOX-carrier nanoparticles have a high drug loading capacity and favourable release property for magnetic drug targeting. The drug release kinetics followed the Korsmeyer–Peppas model at pH 4.2, while at pH 7.4 the zero order model was fitted the best. The drug release mechanism followed super-case II transport in acidic and basic medium. The samples were characterized by XRD, SEM, TEM, FTIR, and UV–Vis.

Keywords: magnetite drug targeting; functionalization; poly(acrylic acid); anticancer drug; controlled delivery; release kinetic studies.

INTRODUCTION

Recently, Fe_3O_4 magnetic nanoparticles (MNs) have been widely used in biology and medicine in fields such as immunoassay, drug delivery and magnetic resonance imaging (MRI) due to their favourable characteristics, such as chemical stability, low toxicity and ultra-fine size, *etc.*[1,2] Bare magnetite nanoparticles on account of their large surface area/volume ratio tend to agglomerate. To prevent agglomeration, a variety of polymeric coatings have been applied to nanoparticles.[3,4] Of these polymers, poly(acrylic acid) (PAA) has been identified as being highly effective.

* Corresponding author. E-mail: reyhan.omidirad@gmail.com
doi: 10.2298/JSC121225041O

The PAA shell reduces the interactions of the electrostatic particles and as a result significantly augments the stability of the diffusion colloid. Poly(acrylic acid) is an aqueous soluble polymer with a high density of reactive functional groups, well known for its biocompatibility and widely used in drug delivery systems, especially as a mucoadhesive drug carrier.[5] Surface-modified Fe_3O_4 nanoparticles have been explored as drug carriers. Doxorubicin (DOX) is an efficient anti-neoplastic agent commonly used in the treatment of a variety of cancers, such as leukaemia, ovarian cancer and, especially, late-stage breast cancer.[6] The clinical use of DOX is limited by the resistance developed by cancer cells and the strong side effects of DOX, namely dose-dependent cardiotoxicity.[7] Drug targeting (drug delivery to the tumour site) can prevent side effects and increase the cytotoxicity of doxorubicin. One of the possible approaches for drug targeting is delivery using magnetic nanoparticles, which can be retained in a tumour by application of an external magnetic field.[8,9]

In this research, one kind of novel nano-scale carrier for doxorubicin was prepared using Fe_3O_4 nanoparticles as the core, PAA as a polymeric shell and doxorubicin as a drug to form drug-loaded magnetic nanoparticles.

EXPERIMENTAL

Materials

All chemicals were of analytical grade and used without further purification, iron(III) chloride hexahydrate ($FeCl_3 \cdot 6H_2O$, Merck), poly(acrylic acid) 5000 (PAA-5000, Polysciences), anhydrous sodium sulphite (Na_2SO_3, Merck), ferrous ammonium sulphate ($(NH_4)_2Fe(SO_4)_2 \cdot 6H_2O$, Carlo Erba), doxorubicin hydrochloride (DOX, Pharmacia Italia SpA, Milan, Italy), tris hydroxymethyl aminomethane (Tris, Merck).

Chemical synthesis of Fe_3O_4 nanoparticles

Fe_3O_4 nanoparticles were prepared using the reduction–precipitation method.[10] Briefly, aqueous solutions of 0.3M $FeCl_3 \cdot 6H_2O$ (45 ml) and 2 M HCl (0.5 ml) were placed into a 200-ml glass beaker and subsequently aqueous solution of 0.3 M Na_2SO_3 (15 ml) was put into the beaker under stirring; Meanwhile, in another clean 1000-ml glass beaker, 50.8 ml of concentrated ammonia was diluted to a total volume of 800 ml with deionised water. In the smaller beaker, the colour of solution could be seen to turn into red from light yellow immediately upon mixing Fe^{3+} and SO_3^{2-}, implying the formation of complex ions. Then, when the colour had returned from red to yellow, the solution was quickly poured into the dilute ammonia solution under intensive stirring. After continuation of the stirring for 30 min, the beaker with the suspension was placed on a permanent magnet. A black powder could be observed rapidly precipitating on the bottom of the beaker. The supernatant was discarded and fresh water added to the beaker. This technique was performed 5 times until a great part of the ions in the suspension had been removed. The powders were extracted by filtration and dried at room temperature.

Preparation of PAA-functionalized magnetite nanoparticles

The as produced nanoparticles were washed 3 times in absolute ethanol, centrifuged, and vacuum-dried overnight. Then, the dried nanoparticles were dispersed in deionised water using ultrasound. A solution of PAA in deionised water were added into the suspension under

stirring, and stirred for 24 h. The Fe_3O_4:PAA mass ratio was 1:2. The product was washed with deionised water and freeze-dried under vacuum at –20 °C for 24 h.

Preparation of DOX–SPION

A solution of DOX–Fe^{2+} complex of 1.5:1 drug:iron molar ratio was obtained by adding an aqueous solution of $(NH_4)_2Fe(SO_4)_2 \cdot 6H_2O$ to DOX in tris buffer pH 7.6. Then the DOX––Fe^{2+} complex was incubated in the dark with the PAA-coated SPION (PS), the mass ratio of DOX:PS was 0.31 mass %. After incubation for 30 min, the drug-loaded PS were separated by centrifugation at 19000 rpm for 15 min (4 °C). Finally, the resulting solid product was washed with ice-cold fresh aqueous buffer pH 7.6 and used immediately afterwards.

Drug loading determination

The DOX loading, %, was defined as the weight fraction of the drug in doxorubicin-loaded PS (DLPS). To measure the loaded drug, particles equivalent to 5 mg were accurately weighed and re-suspended for 20 min in acetate buffer (pH 4.0), conditions that lead to complete dissociation of the DOX–Fe^{2+} complex and therefore to the release of 100 % of DOX. Then, the sample was centrifuged and the DOX concentration measured by means of UV–Vis using the DOX absorbance at 480 nm.

The drug-loading capacity, %, was determined using the following equation:

$$\text{Drug loading} = 100\frac{W_1 - W_2}{W_1} \tag{1}$$

where W_1 is the initial weight of DOX that was incorporated into the PS and W_2 is the weight of free drug (unincorporated DOX). Each determination was performed in triplicate.

Kinetics of drug release

In order to understand the kinetics and mechanism of drug release from DLPS, the drug-loaded nanoparticles were suspended in 50 ml of acetate buffer (pH 4.2) or phosphate buffer (pH 7.4) at 37 °C for 8 h under constant stirring (200 rpm) by a mechanical stirrer. At given time intervals, 2 mL of the release medium was removed for analysis and replaced with 2 mL of same buffer solution. The concentration of drug released was determined from the absorbance at 480 nm (measured using a UV–Vis spectrophotometer) and previously established calibration curves.

The results of the *in vitro* drug release study were fitted with zero order model (cumulative drug release *vs*. time), first order model (ln (cumulative drug remaining) *vs*. time), Higuchi model (cumulative drug release *vs*. $t^{1/2}$), Hixson–Crowell model (cube root of drug remaining in the matrix *vs*. time) and the Korsmeyer–Peppas model (log (cumulative drug released) *vs*. log *t*). The kinetic model that best fitted the dissolution data was evaluated by comparing the regression coefficient (r^2) values of the various models. The "*n*" (release exponent) value of the Korsmeyer–Peppas model used to characterize the different mechanisms of drug release from polymeric systems. For nanoparticles of spherical shape, values of $n \leq 0.43$ mean Fickian diffusion, between 0.43 to 0.85 mean anomalous (non-Fickian) diffusion, $n = 0.85$ for case II transport and $n > 0.85$ for super-case II transport.[11] To determine the drug release mechanism, first 60 % of the drug release data was fitted to the Korsmeyer–Peppas model.

Characterization of nanoparticles

Powder X-ray diffraction (XRD) patterns were acquired from dried nanoparticle samples employing a Rigaku D/max rA X-ray diffractometer using Cu$K\alpha$ radiation. A Philips-CM120

transmission electron microscope (TEM) at an accelerating voltage of 120 KV and a Hitachi S-4160 field emission scanning electron microscope (FE-SEM) at an accelerating voltage of 15 kV were used to observe the morphologies of the Fe_3O_4 MNs and PS. Fourier transform infrared (FTIR) spectra were taken on a Bruker FTIR spectrometer (Tensor 27) and the UV–Vis absorption spectra were recorded using a Camspec-M350 double beam spectrophotometer.

RESULTS AND DISCUSSION

XRD Analysis

The XRD patterns of the bare Fe_3O_4 and PS are shown in Fig. 1. These patterns detect the nanocrystalline structure of the nanoparticles and the mean particle size. The seven diffraction peaks visible in both patterns are consistent with the diffraction peaks of (220), (311), (400), (422), (511), (440) and (533), ascertained by comparison with Joint Committee on Powder Diffraction Standards (JCPDS card, File No. 79-0418). These coincidences suggests that the crystalline structure of Fe_3O_4 did not change on modification of the particles with PAA chains and shows that the PAA coating occurred only at the surface of Fe_3O_4 MNs and resulted in no detectable chemical/physical change in bulk of the nanoparticles.

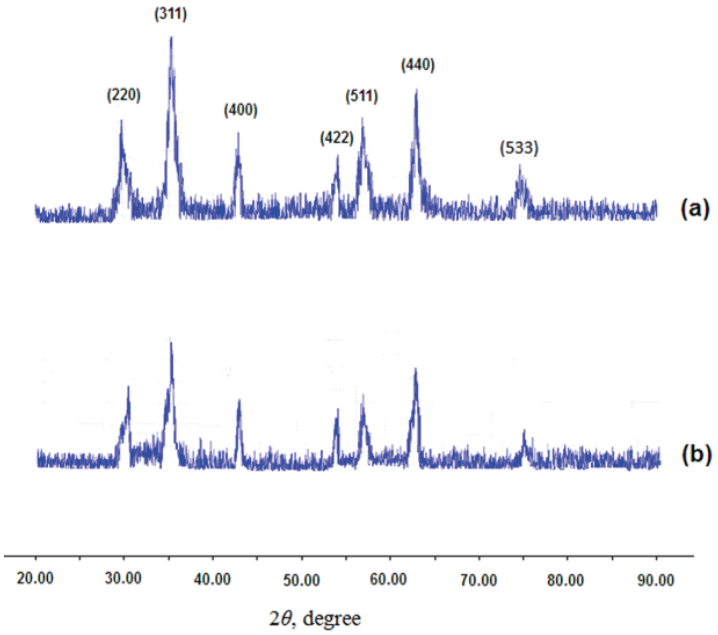

Fig. 1. XRD Patterns of a) uncoated Fe_3O_4 MNs and b) PAA-coated Fe_3O_4 MNs.

Particle sizes can be quantitatively evaluated from XRD data using the Debye–Scherrer equation.

$$D = K\lambda/(\beta\cos\theta) \quad (2)$$

where, K (=0.89) is the Scherrer constant, λ is the X-ray wavelength, β is the peak width at half-maximum height and θ is the Bragg diffraction angle.

The crystallite sizes of the Fe_3O_4 and PS were found to be about 6 and 11 nm, respectively.

FE-SEM and TEM analysis

The morphologies of magnetic nanoparticles were investigated by FE-SEM and TEM, as shown in Fig. 2a–d. These images showed that the prepared nanoparticles had regular spherical shape and a core–shell structure. Due to large specific surface area and high surface energy, some bare magnetite nanoparticles were aggregated (Fig. 2a). However, after being coated with PAA, the nanoparticles were well dispersed (Fig. 2b). Therefore, PAA coating reduced the aggregation and enhanced the particle dispersion. It is an important factor in drug delivery applications that nanoparticles are individually dispersed and are not agglomerated because aggregation would reduce the effective magnetization of nanoparticles and cause difficulties during drug delivery to the desired site.[12]

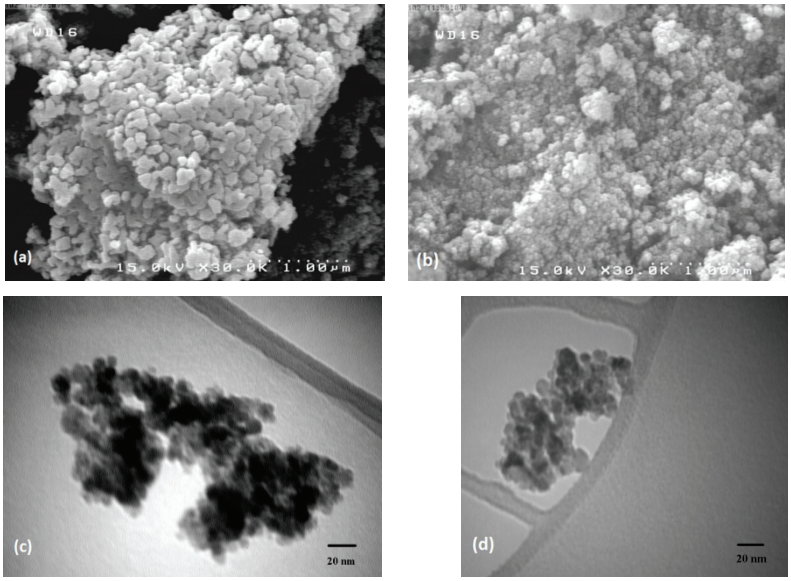

Fig. 2. FE-SEM Images of a) uncoated Fe_3O_4 MNs, b) PAA coated Fe_3O_4 MNs and TEM images of c) uncoated Fe_3O_4 MNs and d) doxorubicin-loaded PAA-coated Fe_3O_4 MNs.

FTIR Analysis

The FTIR spectra of bare Fe_3O_4 MNs (a) and PS (b) are shown in Fig. 3. The IR peak at approximately 603 cm^{-1} was assigned to Fe–O,[13] and the peak at

3434 cm^{-1} was attributed to the stretching vibrations of –OH, which resulted from OH^{-} absorbed by Fe_3O_4 nanoparticles. Moreover, Fig. 3b shows additional peak of the C=O stretching band at 1710 cm^{-1}, the COO^{-} stretching bands at 1423 and 1554 cm^{-1}, and $–CH_2–$ bending band at 1492 cm^{-1}. These results suggested that the Fe_3O_4 MNPs had been successfully coated by PAA-5000.

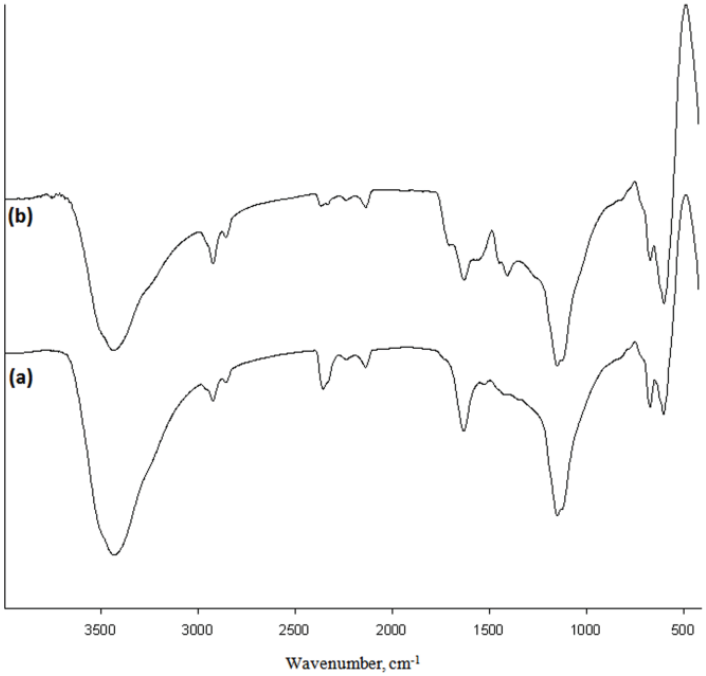

Fig. 3. FTIR Spectra of a) bare Fe_3O_4 MNs and b) PAA-coated Fe_3O_4 MNs.

Drug loading and in vitro *release analysis*

The drug loading efficiency of DLPS was (14.64±0.29). The low values of the standard deviation indicate uniformity of the drug content in the nanocarriers. The drug-loaded nanoparticles were incubated in acetate buffer and phosphate buffer at different pH values to examine the drug release. The chosen pH levels replicated those found in the acidity environment of cancer cells (pH 4.2), as well as blood (pH 7.4). As shown in Fig. 4, the drug release at pH 4.2 was much faster than that at pH 7.4. This is likely due to protonation of the phenol group of DOX in the acidic environment, which leads to the faster dissociation of the DOX–iron complex.[14]

Kinetic modelling of release data

The regression coefficient (r^2) values for DLPS are tabulated in Table I. The model that gave higher r^2 values was considered as best fit model. Based on the

r^2 values, it was also observed that the release of drug from DLPS at pH 4.2 followed the Korsmeyer–Peppas kinetic model while at pH 7.4, the zero-order kinetic model was best fitted. The '*n*' values of the Korsmeyer–Peppas equation for DLPS suggested that the drug release behaviour was super case II transport at the two pH values. These experiments were performed twice.

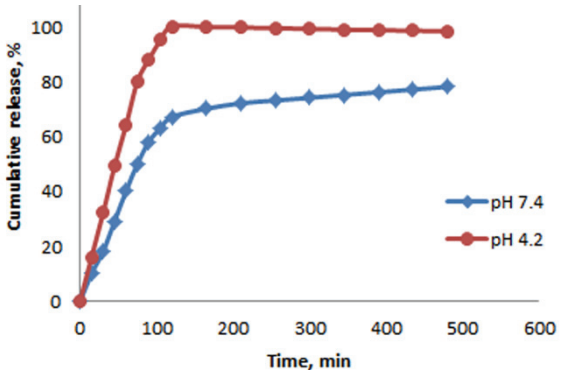

Fig. 4. *In vitro* drug release of DLPS into pH 4.2 and 7.4 solutions

TABLE I. *In vitro* release kinetics studies of DLPS

pH	Regression coefficient, r^2, values					Release exponent "*n*" values
	Zero order	First order	Higuchi	Hixson Crowell	Korsmeyer–Peppas	
4.2	0.9998	0.9802	0.9946	0.9919	0.9999	1.0058
	0.9987	0.9871	0.9938	0.9883	0.9999	1.0193
7.4	0.9986	0.9950	0.9910	0.9973	0.9981	1.0085
	0.9991	0.9906	0.9927	0.9964	0.9973	1.0047

CONCLUSIONS

Spherical magnetite particles, prepared using a reduction–precipitation method, were successfully modified with PAA and confirmed by FTIR spectroscopy. Based on X-ray diffraction, introduction of the PAA coating did not affect the crystalline structure of Fe_3O_4, whereas, based on FE-SEM, it enhanced the uniform dispersion of the nanoparticles. Drug loading was confirmed by UV-Vis and *in vitro* release behaviour was investigated. Approximately 78 % of DOX was released into phosphate buffer, pH 7.4, within 8 h but up to 100 % of drug was released at pH 4.2 within approximately 2 h. At pH 4.2, Korsmeyer–Peppas kinetics of drug release were observed while at pH 7.4, drug release kinetics followed the zero order model. The values of the release exponent "*n*" suggested a super-case II transport release mechanism in both phosphate and acetate buffer.

И З В О Д

ПРИПРЕМА И *IN VITRO* ИСПИТИВАЊЕ БРЗИНЕ ОТПУШТАЊА ДОКСОРУБИЦИНА ИНКАПСУЛИРАНОГ У НАНОЧЕСТИЦАМА МАГНЕТИТА ПРЕКРИВЕНИМ ПОЛИАКРИЛНОМ КИСЕЛИНОМ

REYHAN OMIDIRAD, FARZANEH HOSSEINPOUR RAJABI и BAHMAN VASHEGHANI FARAHANI

Department of Chemistry, Faculty of Science, Imam Khomeini International University, Qazvin, Iran

Предмет овог рада је добијање сферичних, супермагнетних наночестица оксида гвожђа, средњег пречника 6 nm, методом редукционе преципитације. Површина наночестица је обложена поли-акрилном киселином 5000, након чега је у честице инкапсулиран лек доксорубицин. Степен инкапсулације лека износио је 14,64±0,29. Ослобађање лека из наночестица праћено је *in vitro* током 8 h у два система са различитим pH вредностима (4,2 и 7,4). Отпуштање лека при pH вредности од 4,2 (100 % лека је ослобођено током 2 h) значајно је брже од отпуштања на pH 7,4 (~78 % током 8 h). Ови резултати указују на то да добијене наночестице имају потенцијал као носачи доксорубицина у системима за контролисано отпуштање под дејством магнетног поља. Кинетика ослобађања лека из наночестица описана је Korsmeyer–Peppas моделом у раствору pH 4,2, док је процес у раствору pH 7,4 могуће описати кинетиком нултог реда. Сви узорци су окарактерисани коришћењем различитих аналитичких метода: XRD, SEM, TEM, FTIR и UV–Vis.

(Примљено 25. децембра 2012, ревидирано 12. марта 2013)

REFERENCES

1. J. Dobson, *Drug. Dev. Res.* **67** (2006) 55
2. S. I. Park, J. H. Kim, J. H. Lim, C. O. Kim, *Curr. Appl. Phys.* **8** (2008) 706
3. Y. Zhang, N. Kohler, M. Zhang, *Biomaterials* **7** (2002) 1553
4. E. Osterberg, K. Bergstrom, K. Holmberg, *Colloids Surfaces, A* **77** (1993) 159
5. K. Burugapalli, V. Koul, A. K. Dinda, *J. Biomed. Mater. Res., A* **68** (2004) 210
6. E. M. Hoke, C. A. Maylock, E. Shacter, *Free Radical Biol. Med.* **39** (2005) 403
7. A. Bast, H. Kaiserová, G. J. M. Den Hartog, G. R. M. M. Haenen, W. J. F. Van Der Vijgh, *Cell Biol. Toxicol.* **23** (2007) 39
8. V. P. Torchilin, *Adv. Drug Deliv. Rev.* **58** (2006) 1532
9. A. S. Lübbe, C. Alexiou, C. Bergemann, *Surg. Res.* **95** (2001) 200
10. S. Qu, H. Yang, D. Ren, S. Kan, G. Zou, D. Li, M. Li, *J. Colloid Interface Sci.* **215** (1999) 190
11. J. Siepmann, F. Siepmann, *Int. J. Pharm.* **364** (2008) 328
12. J. Zhang, S. Rana, R. S. Srivastava, R. D. K. Misra, *Acta Biomater.* **4** (2008) 40
13. J. Ge, Y. Hu, M. Biasini, C. Dong, J. Guo, W. P. Beyermann, Y. Yin, *Chem. Eur. J.* **13** (2007) 7153
14. E. Munnier, S. Cohen-Jonathan, C. Linassier, L. Douziech-Eyrolles, H. Marchais, M. Soucé, K. Hervé, P. Dubois, I. Chourpa, *Int. J. Pharm.* **363** (2008) 170.